TECHNICAL PAPER

Effect of Notch Root Radius on the Apparent Fracture Toughness in CNT and Carbon Fiber Reinforced, Epoxy-Matrix Hybrid Composite

K. Chandra Shekar · M. Naveen Kumar ·
P. K. Subramanian · Anil Kumar ·
B. Anjaneya Prasad · N. Eswara Prasad

Abstract Significantly improved fracture resistance (in terms of fracture toughness) can be imparted to monolithic materials by adopting composite design methodology based on fiber and nano particulate reinforcement technology. The present work describes the fracture behaviour of one such reinforced material; in this case, carbon fiber (C_f)- and carbon nanotube (CNT)- reinforced epoxy composite. The C_f and CNT reinforced, epoxy-matrix hybrid composite in longitudinal and transverse orientations with varied finite notch root radii (in the range of 120–750 μm) are subjected to mode-I (tensile) fracture. The fracture toughness/resistance (K_Q) of the material is then evaluated and analyzed by investigating the influence of varying notch root radii in longitudinal and transverse orientations. Such an analysis has revealed that the present unidirectional epoxy hybrid composite exhibits a critical notch root radius of 270 μm in longitudinal and 390 μm in transverse orientation.

1 Introduction

Advanced materials such as continuous fiber-reinforced polymer matrix composites offer significant enhancements in a variety of properties, as compared to their bulk, monolithic counterparts. These properties include primarily the tensile stress and flexural stress to fracture resistance/toughness. These properties make such composites attractive for structural applications in the aerospace industry owing to cost benefits from potential weight and fuel savings, though the material cost of those very composites are significantly higher. Till date most of the work reported is confined to the study of the fracture behaviour of such materials under mode-I (tensile) loading conditions [1–5]. However it is more realistic to study fracture behaviour under mixed-mode loading conditions since in most practical situations, structures are subjected to mixed-mode loading. Further, even the specimens loaded initially under mode-I loading, will meander significantly and result in conditions that are of mixed-mode I/II or I/III loading. Under such circumstances, it is noteworthy to evaluate the mixed-mode fracture resistance of these materials. In order to do that, notches of finite root radius have to be used [6, 7]. This is because fatigue pre-cracking is not possible in this composite. Hence, the effect of finite notch root radius is evaluated and reported in the present study, in case of C_f

K. Chandra Shekar
Department of Mechanical Engineering, Vignan Institute of Technology and Science, Deshmukhi, Hyderabad 508284, India

M. Naveen Kumar · P. K. Subramanian
Department of Metallurgical and Materials Engineering, Mahatma Gandhi Institute of Technology, Gandipet, Hyderabad 500075, India

A. Kumar
Advanced Systems Laboratory, DRDO, PO Kanchanbagh, Hyderabad 500058, India

B. Anjaneya Prasad
Department of Mechanical Engineering, Jawaharlal Nehru Technological University, Hyderabad 500085, India

N. Eswara Prasad (✉)
Regional Centre for Military Airworthiness (Materials), CEMILAC, DRDO, PO Kanchanbagh, Hyderabad 500058, India
e-mail: nep@cemilac.drdo.in

and CNT reinforced epoxy matrix hybrid composite both longitudinal and transverse orientations. Also the fracture mechanism and the nature of fracture in this unidirectional hybrid composite are evaluated, reported and discussed. The very purpose of present experimental investigation is to demonstrate the in plane anisotropy and varied fracture behaviour in the two orthogonal directions of the hybrid composite. The present study is the first instance where fracture behaviour of newly developed hybrid composite is being reported. Limited experiments indicate the trend of the results; future work is expected to establish the generalization after verifying the repeatability of the experiments.

2 Experimental Details

2.1 Processing of the Material

Unidirectionally wound carbon fibers are the reinforcement in a polymer matrix of epoxy resin mixture of diglycidyl ether of bisphenol-A (DGEBA) and CNT. The synthesis is made through conventional hand lay-up (HLU) technique [8]. The densification and curing process is carried out in a muffle furnace in three heat treatment cycles. The final material obtained had a thickness of 3.4 mm, and a density of 1.56 g/cc, with volume fiber fraction of 82 %.

2.2 Specimen Preparation

Mode-I fracture toughness specimens were machined with notches oriented in longitudinal and transverse orientations and pertain to the geometry of a single edge notch beam (SENB) specimen as described in ASTM D5045-99 [9]. The notches with different notch root radii were introduced by means of Isomet low speed cutting saw using 0.15 and 0.3 mm thick diamond wafer blades by progressive cutting. Notch root radius measurements were made with the help of a profile projector.

2.3 Fracture Toughness Testing

All the fracture toughness tests were conducted on a computer controlled, servo hydraulic Instron 5600R test system using a self articulating 3 point bend fixture. The tests were conducted at ambient temperature ($\sim$23 °C) and in laboratory air atmosphere. The load–displacement plots thus obtained were analyzed to obtain various measures of fracture resistance, and the results are presented and discussed in the following sections. Fracture toughness tests were carried out under ramp control speed of 0.5 mm/min and the load versus crack opening displacements are recorded, as per ASTM standard D5045-99 [9].

3 Results and Discussion

3.1 Notch Profiles

Notches of fixed length maintaining an a/W ratio of 0.45–0.55 and varying notch root radius (ρ) were introduced using diamond wafer blades of thickness varying from 0.15 to 0.3 mm, mounted on a standard Isomet low speed Saw cutting machine. Notches of higher root radius too were introduced by the same Isomet by progressive cutting. The notches thus introduced were found to have finite root radius (ρ) typically of the orders varying from 120 to 750 μm. The ρ values were determined experimentally using Delta TM 35 x–y profile projector. It should be noted here that though the Isomet wafer blades of significantly lower (0.15 mm) thickness were used, its cutting characteristics/behaviour of the present hybrid composite is such that higher notch root radius (ρ) resulted. In homogenous materials the ideal cutting behaviour is expected to result in $\rho = 0.5$–0.6T, where T is the thickness of the Isomet blade. The crack lengths (a/W ratio) were maintained nearly 0.45 and 0.5 times the specimen width in longitudinal and transverse orientations respectively, as specified in the ASTM standard D5045-99 [9] for the determination of K_{Ic} values.

3.2 Load–Displacement Data

The load–displacement data obtained for longitudinal and transverse orientations are shown in Figs. 1 and 2 respectively. These load–displacement data for the two test orientations are obtained for specimens with different notch root radii (ρ). The data regarding the notch root radius and specimen dimensions along with the obtained apparent fracture toughness for the specimen designation (i.e., L1, L2 and T1, T2 etc.) are given in Tables 1 and 2. Absolute values of crack length (a), specimen width (W) are given along with normalized values of a/W. Though six tests with nearly same a/W values and different ρ values were conducted in the longitudinal orientation, for the sake of clarity and close values of ρ in certain conditions, only four load–displacement plots are included in Fig. 1. On the other hand, all six load–displacement plots obtained are included in Fig. 2 for the transverse orientation.

The load initially was found to increase linearly with the displacement in all the cases (Figs. 1, 2). This corresponds to the stage in which the specimen largely experiences mostly elastic stresses. Followed by this stage, the crack extension takes place in an unstable manner. This is reflected in the sudden decrease in the load with increase in the displacement, before the crack arrest takes place. The load–displacement data there after show distinctively different characteristics of crack extension in the two notched orientations.
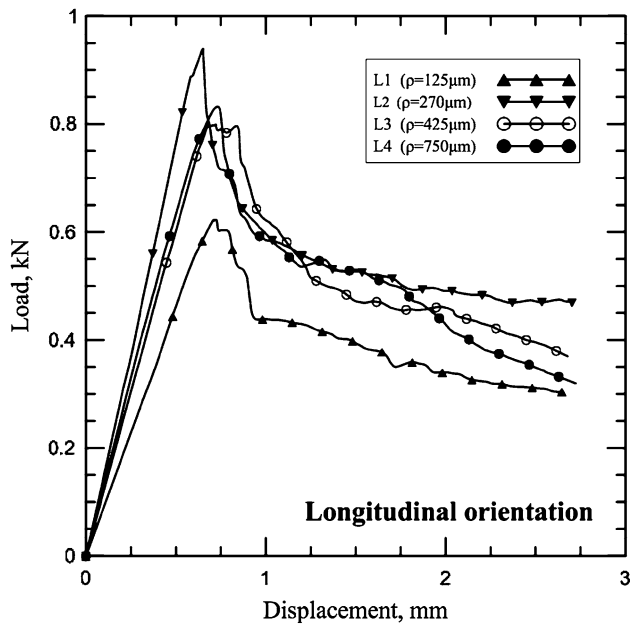
Fig. 1 Load–displacement data obtained in longitudinal orientation with varying finite notch root radius (125–750 μm)
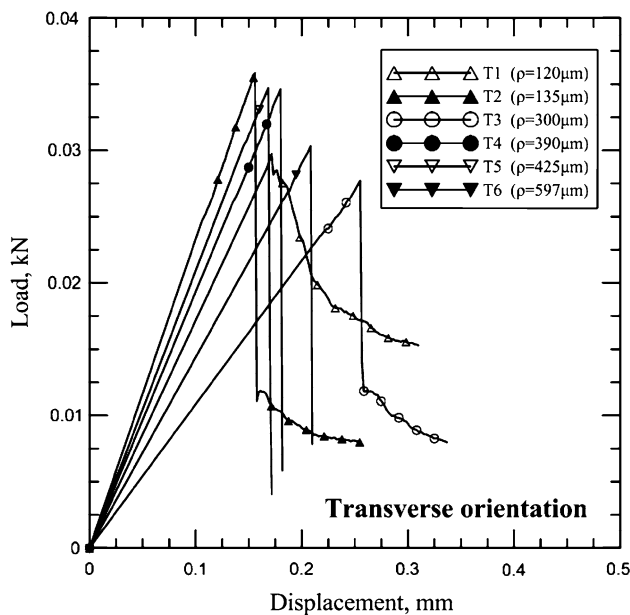

Fig. 2 Load–displacement data obtained in transverse orientation with varying finite notch root radius (120–597 μm)

The material in the longitudinal orientation shows initially a steep and later a gradual and continuous fall in the load with increase in the displacement (Fig. 1). Such behaviour is seen in all the specimens with varying notch root radius from 125 to 750 μm. This behaviour indicates the gradual extension of the crack front. However, it can be observed that specimens with lower root radius (L1 in Fig. 1) show lower extent of steep load drop compared to those with higher notch root radius. This is because the

material exhibits lower K_Q due to the presence of a sharper notch (L1 in Fig. 1 with ρ = 125 μm). Eventually all the specimens show a near-saturation in the variation of load with increase in displacement after a displacement of the order of 1 mm. In this case, the fiber bundles undergo significant bending without breakage and crack extension essentially occurs along the fiber/matrix interface.

On the other hand, the specimens in the transverse orientation show a sudden load drop with increase in displacement (Fig. 2). This behaviour is observed due to the absence of fibers during crack extension and represents solely the toughness of matrix. Specimens in transverse orientation show a near complete mode-I fracture with predominant matrix cracking, leading to significant drop in load after specimens attain maximum load. This results in mode-I crack extension in the initial stage and mixed-mode fracture in later stages comprising mode-I and mode-II components. It should be noted here that the extension of crack under mixed mode I/II is significantly lower in transverse specimens as compared to longitudinal specimens. This is because extensive crack extension in longitudinal specimens occurs with predominant fiber bundle breakage leading to relatively large extent of crack extension along fiber/matrix interface. The nature of load–displacement diagrams is vastly different for the two test orientations of the material. However up to and at crack initiation their nature is similar except for ρ = 425 μm and beyond in longitudinal orientation where crack extension occurs at high 'K' values. Interestingly this value of 425 and 750 μm notch root radius are beyond the critical notch root radius of the material in that test orientation.

3.3 Effect of Notch Root Radius

The apparent fracture toughness (K_Q) as a function of the notch root radius for the two orientations tested is summarized and the data are included in Table 1. It can be clearly inferred that the specimens with lower notch root radius (L1 with ρ = 125 μm) exhibits lower apparent fracture toughness (20.74 MPa$\sqrt{}$m) and the value increases with increase in the root radius (24.27 MPa$\sqrt{}$m for L4 with ρ = 750 μm). The presence of sharper notch facilitates the easy propagation of the crack which results in lesser amount of energy absorption. The results obtained in transverse orientation too show a similar trend. The higher energy absorbed in ρ > 125 μm is due to crack extension from relatively one blunt initial crack.

Crack extension with blunt notches was extensively studied [10, 11], though the same is not reported till date in case of epoxy hybrid composites. In such cases crack extension takes place under critical strain controlled behaviour, the variation of K_Q with the square root of notch root radius should be linear. This is verified with the data

Table 1 Effect of notch root radius on apparent fracture toughness (K_Q) of longitudinal and transverse orientation

Specimen No.	Thickness of Isomet blade used (μm)	Notch root radius (ρ) (μm)	Notch root radius ($\sqrt{\rho}$) ($\sqrt{\mu m}$)	Fracture toughness, K_Q (MPa$\sqrt{m}$)
Longitudinal orientation				
L1	150	125	11.18	20.74
L2	150	270	16.43	19.80
L3	300	425	20.61	24.22
L4	300	750	27.38	24.27
L5	150	150	12.25	20.60
L6	300	575	23.98	26.99
Transverse orientation				
T1	150	120	10.95	0.90
T2	150	135	11.61	1.01
T3	150	300	17.32	0.91
T4	300	390	19.74	0.93
T5	300	425	20.61	1.05
T6	300	597	24.43	1.50

Table 2 Apparent fracture toughness (K_Q, MPa$\sqrt{m}$) data of the C_f-CNT reinforced epoxy hybrid composite

Specimen No.	W (mm)	B (mm)	a (mm)	a/W	f(a/W)	P_Q (N)	P_{max} (N)	K_Q (MPa$\sqrt{m}$)	K_{max} (MPa$\sqrt{m}$)
Longitudinal orientation									
L1	7.50	3.21	3.40	0.45	9.27	622	623	20.74	20.77
L2	8.41	3.19	3.29	0.40	6.27	924	939	19.80	20.12
L3	8.28	3.28	3.70	0.45	9.06	798	801	24.22	24.31
L4	8.40	3.21	3.80	0.45	9.19	777	830	24.27	25.92
L5	8.25	3.07	4.15	0.50	10.65	540	561	20.60	21.40
L6	7.87	3.07	4.31	0.55	12.44	591	600	26.99	27.40
Transverse orientation									
T1	10.05	3.44	5.30	0.52	11.36	27.4	29.7	0.90	0.98
T2	8.43	3.75	4.10	0.48	10.00	34.7	35.8	1.01	1.04
T3	7.98	3.47	3.99	0.50	10.65	26.5	27.7	0.91	0.95
T4	8.03	3.80	3.78	0.47	9.70	32.6	34.6	0.93	0.98
T5	8.30	3.63	4.15	0.50	10.65	32.4	34.7	1.05	1.12
T6	7.96	3.78	3.98	0.50	10.65	47.7	49.7	1.50	1.60

W specimen width, *B* specimen thickness, *a* crack length, P_Q conditional load for onset of fracture, P_{max} maximum load in the load–displacement curve, K_Q apparent fracture toughness, K_{max} maximum stress intensity factor, $f(x) = 6x^{\frac{1}{2}}\left(\frac{[1.99-x(1-x)(2.15-3.93x+2.7x^2)]}{(1+2x)(1-x)^{\frac{3}{2}}}\right)$ where $0 < x < 1$ and x = a/W

obtained in the present study for both longitudinal and transverse orientations illustrated in Figs. 4 and 5 respectively. The fracture toughness value in longitudinal orientation was higher than that of the transverse orientation. This is due to the presence of fibers perpendicular to the loading direction in longitudinal and parallel in case of transverse orientation which is evident from the SEM photographs shown in Fig. 3a, b, c, d. It can also be seen that a linear relationship between K_Q and ρ is obtained for both cases until reaching a critical value of notch root radius (ρ_o) below which the value of the apparent fracture

toughness is invariant (Figs. 4, 5) and such invariant K_Q is the material fracture toughness (provided the other condition of validity $B \geq 2.5(K_Q/\sigma_f)^2$, where K_Q is the apparent fracture toughness and σ_f is flexural strength (with an assumption that fracture stress scales with flexural strength)). This critical value of the notch root radius (ρ_o) is approximately equal to 270 μm in case of longitudinal orientation and 390 μm in case of transverse orientation. This implies that in C_f and CNT reinforced epoxy matrix hybrid composites (unidirectional), if the notch root radius is below the critical value then the fracture toughness is
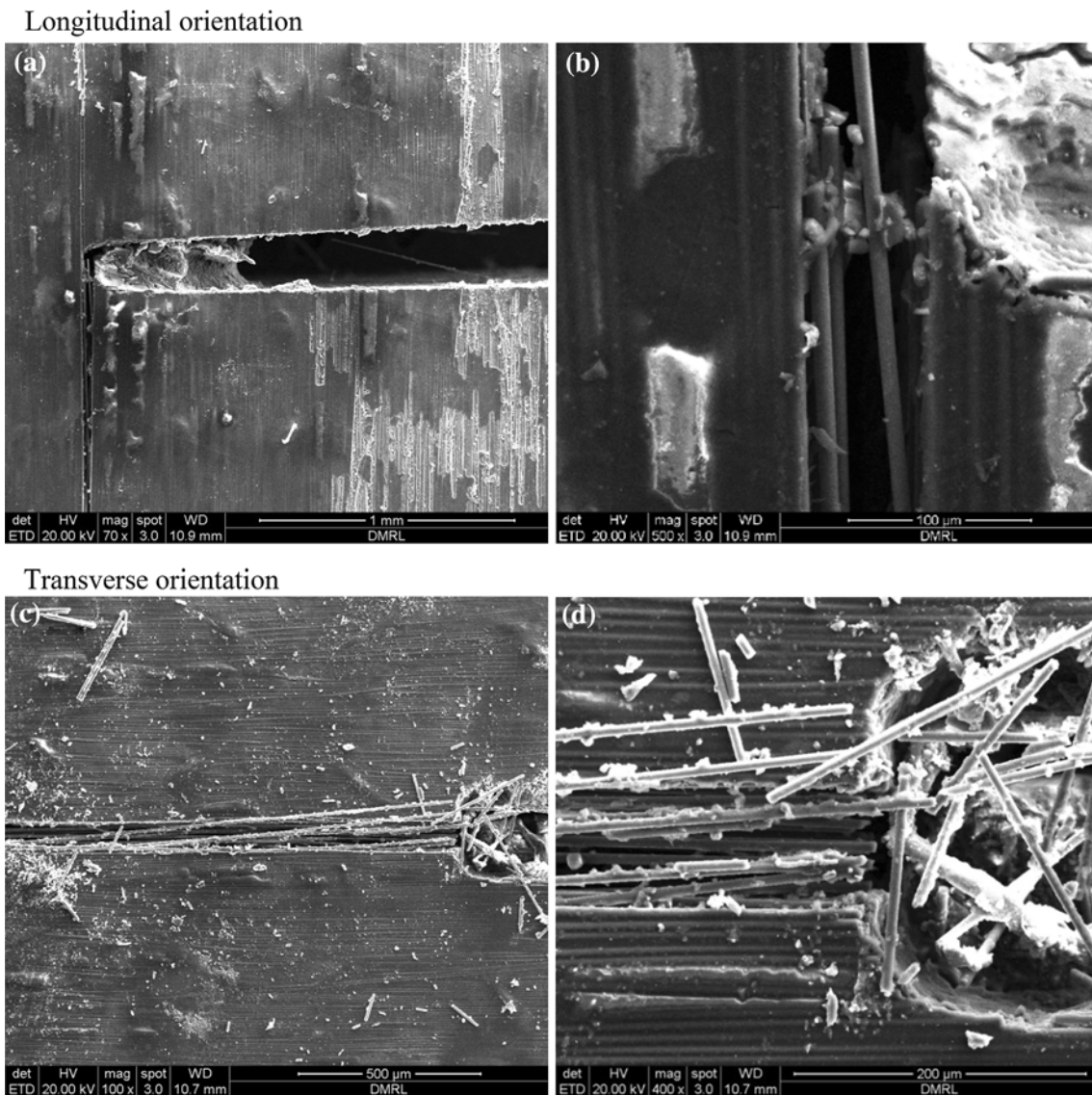
Longitudinal orientation

Transverse orientation

Fig. 3 SEM photographs of fracture toughness tested specimens in longitudinal (**a** low magnification, **b** high magnification) and transverse orientation (**c** low magnification, **d** high magnification)

solely a material property conditional to the fact that the criteria for LEFM and plane strain are satisfied.

3.4 Strain Controlled Fracture

In order to establish if critical strain is controlling fracture in these unidirectional hybrid composites, a fracture mechanics approach suggested by Crowe and Gray [12] can be used. According to them, if there is a linear relationship between δ_i and ρ for $\rho \geq \rho_o$, then the fracture is strain controlled. The crack opening displacement δ_i at crack initiation can be calculated using the relation:

$$\delta_i = \frac{0.49 K_{Ic}^2}{\rho_o E \sigma}, \quad \text{for } \rho > \rho_o \tag{1}$$

where K_{Ic} is the fracture toughness, E is the Young's modulus (16.32 GPa in longitudinal orientation and 15.88 GPa in transverse orientation), σ is the fracture strength (1,084, 38 MPa in longitudinal and transverse orientations respectively) and ρ_o is the critical notch root radius (270 μm for a longitudinal orientation and for transverse orientation is 390 μm). δ_i Versus ρ plots for longitudinal and transverse orientations are shown is Figs. 6 and 7 respectively. It can be seen that in both cases the behaviour is approximately linear although the experimentally measured slope, 0.5563 in longitudinal case and with the theoretical slope obtained using the Eq. (1) which is 0.0183. There exists a linear relation between displacement at the crack initiation and the notch root
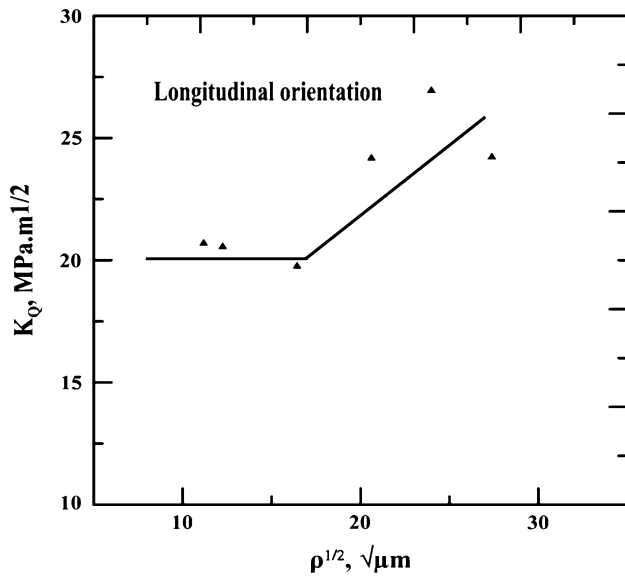
Fig. 4 Variation of apparent fracture toughness with square root of notch root radius in longitudinal orientation
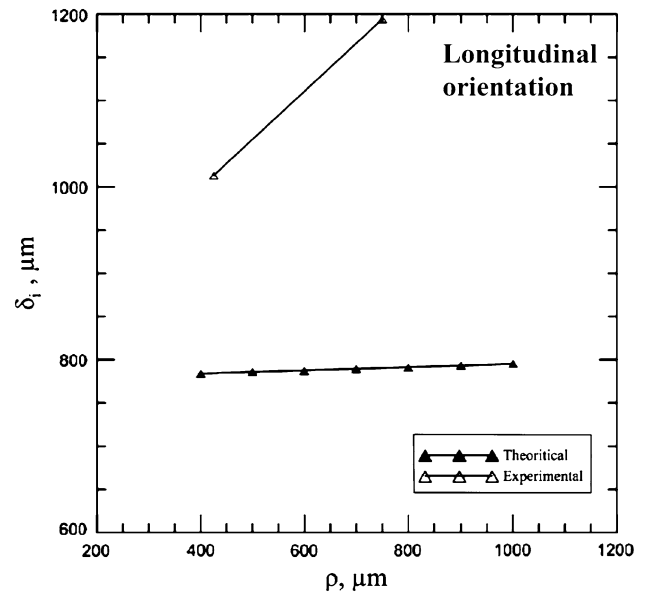

Fig. 6 Variation of crack opening displacement at crack initiation with root radius in longitudinal orientation
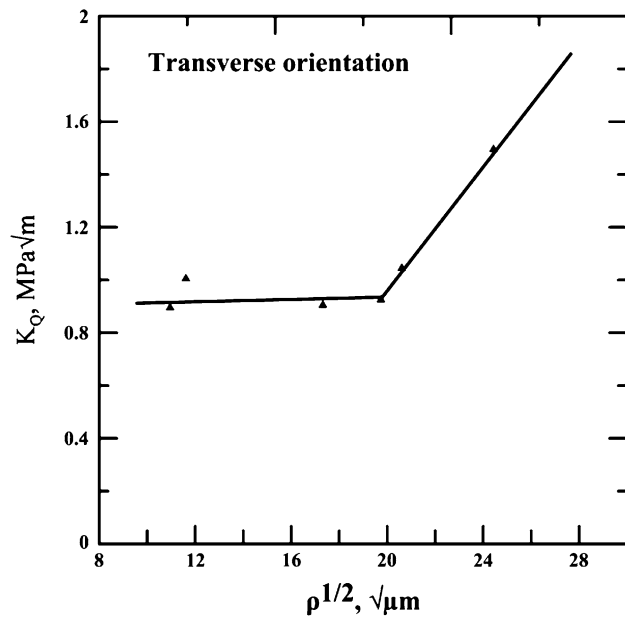

Fig. 5 Variation of apparent fracture toughness with square root of notch root radius in transverse orientation
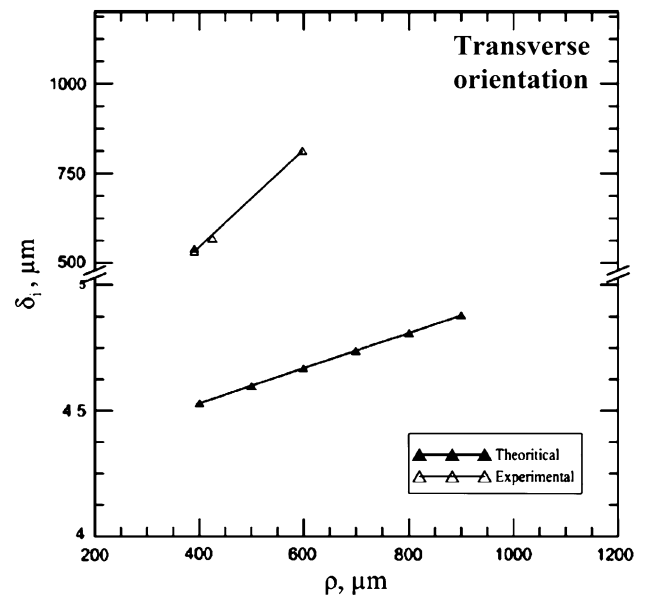

Fig. 7 Variation of crack opening displacement at crack initiation with root radius in transverse orientation

radius; we note that there is wide disparity in the experimentally measured and theoretically estimated slopes of the linear relation values. The slope in transverse case experimentally is 1.353 which does not agree with that of the theoretical slope obtained using the same Eq. (1) which is 0.0007. The disagreement between the theoretical and experimentally measured slopes in longitudinal an transverse cases could be because of the non linearity, like the small scale yielding in metals and the

approximation used in Eq. (1) is not completely valid in this case. These observations imply that the fracture in such composites is strain controlled. The plots shown below represent the linearity between the displacement at the crack initiation and the notch root radius (greater than the critical notch root radius) and thus provide the evidence that the fracture occurred in the material is strain controlled. Fracture indeed is strain controlled in longitudinal orientation as Fig. 6 and Eq. 1 shows a

linear relationship between crack opening displacement and notch root radius. The high value of fracture toughness in this direction is incidental. Similar observation is also found to be true in case of composite in transverse orientation (see data in Fig. 7). However such observations could be quite different as the nature of load–displacement curves are quite drastically different for the two directions. However in case of longitudinal orientation the tensile fracture of the fiber controls the magnitude of fracture resistance, while the same is also true for transverse orientation, but in which case the fracture is controlled by transverse strength of the fiber. However limited fracture toughness data in both orientations suggest that the fracture is largely strain controlled though there are vastly different strengths of the fiber in two orientations. The strain controlled fracture of such composite is very sensitive to Young's modulus and to obtain accurate values, the modulus should be determined experimentally. Therefore the whole results should be relooked, when experimentally determined Young's modulus values are obtained.

4 Conclusions

1. The material in the longitudinal orientation shows initially a steep and later a gradual, continuous fall in the load with increase in the displacement. This is due to the gradual extension of the crack front leading to significant extent of fiber bundle failure.

2. In transverse orientation, a sudden drop in load is observed with increase in displacement. This is because of the failure of matrix as the fibers contribution is minimal. The extent of gradual decrease in load with further increase in displacement is lower in transverse specimens as compared to longitudinal specimens.

3. The apparent fracture toughness is independent of the notch root radius below a critical notch radius of 270 μm for a longitudinal orientation and increases linearly with the square root of notch root radius for ρ greater than 270 μm and ρ_o for transverse orientation is 390 μm.

4. The apparent fracture toughness of the material is nearly 0.94 MPa$\sqrt{m}$ in transverse orientation, whereas the same is nearly 20.27 MPa$\sqrt{m}$ in longitudinal

orientation. Such a large variation in fracture resistance in two directions of same material brings out the fact that crack bridging due to the presence of unidirectional carbon fiber reinforcement is so effective that nearly 20 times higher fracture resistance is imparted to the material as compared to its monolithic matrix epoxy counterpart.

5. Using the fracture mechanics approach suggested by Crowe and Gray, it is determined that the fracture process in such composites is strain controlled.

References

1. Bortz D R, Merino C, Martin-Gullon I, *Composites Science and Technology* **71** (2011) 31.
2. El-Hajjar R, Haj-Ali R, *Engineering Fracture Mechanics* **72** (2005) 631.
3. Solaimurugan S, Velmurugan R, *Composites Science and Technology* **68** (2008) 1742.
4. Melcher R J, Johnson W S, *Composites Science and Technology* **67** (2007) 501.
5. Wong D W Y, Lin L, McGrail P T, Peijs T, Hogg P J, *Composites Part A: Applied Science and Manufacturing* **41** (2010) 759.
6. Kamat S V and Eswara Prasad N, *Scripta Metallurgica et Materialia* **25** (1991) 1519.
7. Vratnica M, Pluvinage G, Jodin P, Cvijović Z, Rakin M, Burzić Z, *Materials & Design* **31** (2010) 1790.
8. Chandra Shekar K, Sai Priya M, Subramanian P K, Anil Kumar, Anjaneya Prasad B and Eswara Prasad N, *Bulletin of Materials Science* (Submitted for Publication).
9. ASTM Standard D 5045-99, *Standard Test Methods for Plane-Strain Fracture Toughness and Strain Energy Release Rate of Plastic Materials*, Annual Book of ASTM Standards vol. 08.02, American Society for Testing and Materials, West Conshohocken (2007).
10. Eugênio de Azevedo Soriano, Sérgio Frascino Müller de Almeida, *Composites Science and Technology* **59** (1999) 1143.
11. Lagace P A, *Composites Science and Technology* **26** (1986) 95.
12. Crowe C R and Gray R A, *Proc. 39th Meeting of High Performance Group* (1984) 157.